GEOPHYSICS, VOL. 63, NO. 1 (JANUARY-FEBRUARY 1998); P. 289–296, 7 FIGS.

A frequency-space 2-D scalar wave extrapolator using extended 25-point finite-difference operator

Changsoo Shin* and Heejeung Sohn‡

ABSTRACT

Finite-difference frequency-domain modeling for the generation of synthetic seismograms and crosshole tomography has been an active field of research since the 1980s. The generation of synthetic seismograms with the time-domain finite-difference technique has achieved considerable success for waveform crosshole tomography and for wider applications in seismic reverse-time migration. This became possible with the rapid development of high performance computers. However, the space-frequency (x, ω) finite-difference modeling technique is still beyond the capability of the modern supercomputer in terms of both cost and computer memory. Therefore, finite-difference time-domain modeling is much more popular among exploration geophysicists. A limitation of the space-frequency domain is that the recently developed nine-point scheme still requires that G, the number of grid points per wavelength, be 5. This value is greater than for most other numerical modeling techniques (for example, the pseudospectral scheme). To overcome this disadvantage inherent in space-frequency domain modeling, we propose a new weighted average finite-difference operator by approximating the spatial derivative and the mass acceleration term of the wave equation. We use 25 grid points around the collocation. In this way, we can reduce the number of grid points so that G is now 2.5. This approaches the Nyquist sampling limit in terms of the normalized phase velocity.

INTRODUCTION

Seismic inversion of the scalar wave equation using implicit finite-difference methods in the space-frequency (x, ω) domain has been employed recently by Pratt and Worthington (1990). Unfortunately, the complex impedance matrices required by implicit finite-difference methods are huge. Therefore, any savings in the number of grid points required in such schemes is of critical importance. In the space-time or (x, t) domain, for a time step Δt or near the stability limit, ten ($G = 10$) or more grid points per wavelength should be used when a second-order finite-difference technique is employed, while a fourth-order $O(\Delta t^2, \Delta x^4)$ scheme requires five grid points per wavelength (Alford et al., 1974). Finite-difference algorithms using higher order terms such as $O(\Delta t^4, \Delta x^{10})$ require three grid points per wavelength, approaching the same level of accuracy as the pseudospectral method (Dablain, 1986). One disadvantage of the space-time (x, t) domain is that for strongly inhomogeneous velocity models, the accuracy depends on the value of the local velocity, while the stability limit is determined by the greatest velocity in the model. The space-frequency domain modeling does not have any stability problem (Marfurt, 1984). In spite of this advantage, the conventional five-point operator in the space-frequency domain (Pratt and Worthington, 1990) requires more grid points ($G = 13$) than the corresponding operators in the space-time domain to achieve the same accuracy. The algorithm developed by Jo et al. (1996) exploited a finite-element–like (Marfurt, 1984) optimal nine-point finite-difference star for the approximation of the Laplacian and the mass acceleration terms, in which an optimal set of coefficients could be found. The nine-point scheme allowed the number of grid points to be reduced from thirteen per wavelength to five or six per wavelength (maintaining the same accuracy).

In this study, we present a new scheme for designing a 25-point operator based on a new averaging method for selecting coefficients. In contrast to the method used to develop the nine-point star, we use a weighted Laplacian operator and mass acceleration term at four different rotation angles to reduce numerical anisotropy. We find coefficients by constructing the overdetermined matrix satisfying the best normalized phase velocity and solve it using a singular-value decomposition

Manuscript received by the Editor July 26, 1995; revised manuscript received May 12, 1997.
*Dept. of Mining and Petroleum Engineering, College of Engineering, Seoul National University, San 56-1, Sinlim-Dong Kwanak-ku, Seoul, Korea. E-mail: css@model.snu.ac.kr.
‡Dong Ah Construction Industrial Co., Ltd. Technology & Research Institute, Fine Chemical Bldg. 4F190-3, Choong Jeong Rd., 2GA SeoDae Mun-Gu, Seoul 120-012, Korea.

method. Numerical analysis indicates that a 25-point finite-difference operator in the forward modeling when solving the 2-D scalar wave equation can reduce the number of grid points down to three points per wavelength in terms of the group velocity, thereby approaching the accuracy of the pseudospectral method.

IMPROVEMENT OF THE ACCURACY BY A 25-POINT AVERAGE FINITE DIFFERENCE SCHEME

In a Cartesian coordinate system, the 2-D scalar wave equation with no damping in the frequency domain is given by

$$\nabla^2 P + \frac{\omega^2}{v^2} P = f(\omega)\delta \cdot (x - x_s)\delta(z - z_s), \qquad (1)$$

where $P(x, z, \omega)$ is the Fourier component of the wavefield pressure, ω is the angular frequency, $v(x, z)$ is the velocity of propagation, $f(\omega)$ is the source function Fourier transform, $\delta(x)$ is the Dirac delta function, and x_s and z_s are the horizontal and vertical coordinates of the source location. The conventional second-order finite-difference approximation to equation (1) is

$$\frac{P_{m+1,n} - 2P_{m,n} + P_{m-1,n}}{\Delta x^2} + \frac{P_{m,n+1} - 2P_{m,n} + P_{m,n-1}}{\Delta z^2} + \frac{\omega^2}{v^2} P_{m,n} = F(\omega)\delta_{sr}, \qquad (2)$$

where Δx and Δz are the finite-difference grid spacing in x- and z-direction, respectively, $P_{m,n}$ is the discretized wavefield at $([x_m, z_n] = [x_0 + (m-1)\Delta x, z_0 + (n-1)\Delta z])$, and δ_{mn} is Kronecker delta, with $\delta_{sr} = 1$ when $s = r$ and $\delta_{sr} = 0$ otherwise. In the case of the extended 25-point average finite-difference star shown in Figure 1, we can have four different finite-difference operators at 0°, 26.6°, 45°, and 63.4°, each approximating the Laplacian in a different coordinate frame:

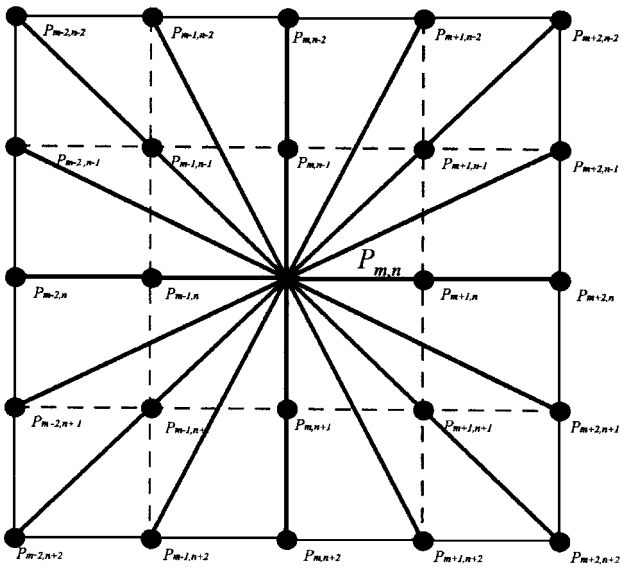

FIG. 1. The 25-point finite-difference computational grid.

$$\nabla^2_{(0)} P = \frac{\partial^2 P}{\partial x_0^2} + \frac{\partial^2 P}{\partial z_0^2},$$

$$\nabla^2_{(26.6)} P = \frac{\partial^2 P}{\partial x_{26.6}^2} + \frac{\partial^2 P}{\partial z_{26.6}^2};$$

$$\nabla^2_{(45)} P = \frac{\partial^2 P}{\partial x_{45}^2} + \frac{\partial^2 P}{\partial z_{45}^2}, \qquad (3)$$

$$\nabla^2_{(63.4)} P = \frac{\partial^2 P}{\partial x_{63.4}^2} + \frac{\partial^2 P}{\partial z_{63.4}^2},$$

where x_θ, z_θ denote the Cartesian grid rotated by θ degrees. Finite-difference approximations to equation (3) for the inner nine-point grid (Figures 2a and 2b) are given by

$$\nabla^2_{(0,\Delta)} P\big|_{x=x_m, z=z_n} = \frac{(P_{m+1,n} + P_{m-1,n} - 4P_{m,n} + P_{m,n+1} + P_{m,n-1})}{\Delta_0^2}, \qquad (4a)$$

$$\nabla^2_{(45,\sqrt{2}\Delta)} P\big|_{x=x_m, z=z_n} = \frac{(P_{m+1,n+1} + P_{m-1,n+1} - 4P_{m,n} + P_{m+1,n-1} + P_{m-1,n-1})}{2\Delta_{45}^2}, \qquad (4b)$$

while approximations using the outer 17-point grid (Figures 2c–2f) are given by

$$\nabla^2_{(0,2\Delta)} P\big|_{x=x_m, z=z_n} = \frac{(P_{m+2,n} + P_{m-2,n} - 4P_{m,n} + P_{m,n+2} + P_{m,n-2})}{4\Delta_0^2}, \qquad (4c)$$

$$\nabla^2_{(45,2\sqrt{2}\Delta)} P\big|_{x=x_m, z=z_n} = \frac{(P_{m+2,n+2} + P_{m-2,n+2} - 4P_{m,n} + P_{m+2,n-2} + P_{m-2,n-2})}{8\Delta_{45}^2}, \qquad (4d)$$

$$\nabla^2_{(26.6,\sqrt{5}\Delta)} P\big|_{x=x_m, z=z_n} = \frac{(P_{m+2,n-1} + P_{m+1,n+2} - 4P_{m,n} + P_{m-2,n+1} + P_{m-1,n-2})}{5\Delta_{26.6}^2}, \qquad (4e)$$

and

$$\nabla^2_{(63.4,\sqrt{5}\Delta)} P\big|_{x=x_m, z=z_n} = \frac{(P_{m+1,n-2} + P_{m+2,n+1} - 4P_{m,n} + P_{m-1,n+2} + P_{m-2,n-1})}{5\Delta_{63.4}^2}. \qquad (4f)$$

Following Jo et al. (1996) in approximating the mass acceleration term, we can approximate the pressure $P_{m,n}$ of the mass

acceleration term in equation (2) by using the eclectic form of a lumped mass at the center node itself and the consistent mass at its neighboring nodes (Marfurt, 1984). We distribute the pressure $P_{m,n}$ of the mass acceleration term in equation (2) at the collocation point and its neighboring points. In our 25-point finite-difference grids, we separated 25-point finite-difference grids into seven difference groups of nodal points as

$$\bar{P}_{(0,0)} = P_{m,n}, \tag{5a}$$

$$\bar{P}_{(0,\Delta)} = P_{m-1,n} + P_{m,n-1} + P_{m+1,n} + P_{m,n+1}, \tag{5b}$$

$$\bar{P}_{(45,\sqrt{2}\Delta)} = P_{m-1,n-1} + P_{m+1,n-1} + P_{m+1,n+1} + P_{m-1,n+1}, \tag{5c}$$

$$\bar{P}_{(0,2\Delta)} = P_{m-2,n} + P_{m,n-2} + P_{m+2,n} + P_{m,n+2}, \tag{5d}$$

$$\bar{P}_{(45,2\sqrt{2}\Delta)} = P_{m-2,n-2} + P_{m+2,n-2} + P_{m+2,n+2} + P_{m-2,n+2}, \tag{5e}$$

$$\bar{P}_{(26.6,\sqrt{5}\Delta)} = P_{m+2,n-1} + P_{m+1,n+2} + P_{m-2,n+1} + P_{m-1,n-2}, \tag{5f}$$

$$\bar{P}_{(63.4,\sqrt{5}\Delta)} = P_{m+1,n-2} + P_{m+2,n+1} + P_{m-1,n+2} + P_{m-2,n-1}, \tag{5g}$$

where the first number in parenthesis indicates the angle of rotation and the second number in parenthesis indicates the distance from the collocation point. Each group of nodal points in equation (5) will have different weighting coefficients and the weighted average of each group will be used to approximation the pressure $P_{m,n}$ in equation (2).

Since each of these approximations to $\nabla^2 P$ and $\bar{P}$ approaches the true value as $\Delta \to 0$, we can approximate $\nabla^2 P$ and $\bar{P}$ in equation (2) by any linear combination of the estimates given by equations (4) and (5). We express this arbitrary linear combination with (yet to be determined) coefficients $a_1 - a_6$, $b_1 - b_7$, thereby obtaining the finite-difference equation

$$\begin{aligned}
&\left(a_1\nabla^2 P_{(0,\Delta)} + a_2\nabla^2 P_{(0,2\Delta)} + a_3\nabla^2 P_{(45,\sqrt{2}\Delta)}\right.\\
&\quad + a_4\nabla^2 P_{(45,2\sqrt{2}\Delta)} + a_5\nabla^2 P_{(26.6,\sqrt{5}\Delta)} + a_6\nabla^2 P_{(63.4,\sqrt{5}\Delta)}\Big)\\
&\quad + \frac{\omega^2}{v^2}\left(b_1\bar{P}_{(0,0)} + b_2\bar{P}_{(0,\Delta)} + b_3\bar{P}_{(0,2\Delta)} + b_4\bar{P}_{(45,\sqrt{2}\Delta)}\right.\\
&\quad \left. + b_5\bar{P}_{(45,2\sqrt{2}\Delta)} + b_6\bar{P}_{(26.6,\sqrt{5}\Delta)} + b_7\bar{P}_{(63.4,\sqrt{5}\Delta)}\right) = 0,
\end{aligned} \tag{6}$$

where the coefficients are additionally constrained by $\sum_{i=1}^{6} a_i = 1$, $b_1 + 4\sum_{i=2}^{7} b_i = 1$.

The object of creating the linear combination given in equation (6) is to combine the dispersion characteristics of each separate finite-difference operator in the most optimal means. This is accomplished by expressing normalized phase and group velocities in terms of the coefficients, and adjusting the

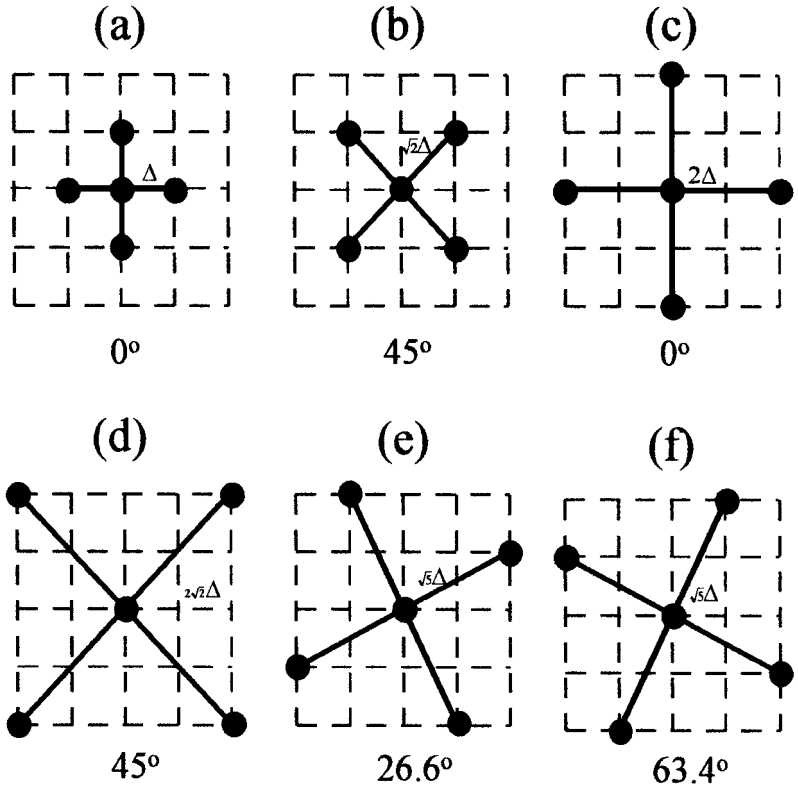

FIG. 2. Five-point Laplacian operators extracted from Figure 1, corresponding to equations (4a)–(4f).

coefficients to keep these normalized velocities as close to unity as possible.

We now perform classical dispersion analysis by assuming a plane-wave solution of the form:

$$P_{(x,z)} = e^{ik(x\cos\theta + z\sin\theta)},$$

where θ is the propagation angle.

Substituting this plane harmonic wave into equations (4)–(6) yields

$$\frac{\omega^R}{V^R} = \frac{L}{M\Delta^2}, \tag{7}$$

where

$$\begin{aligned} L = {} & a_1(4 - 2\cos(2\pi(\sin\theta)/G) - 2\cos(2\pi(\cos\theta)/G)) \\ & + a_2(1 - 0.5\cos(4\pi(\cos\theta)/G) \\ & - 0.5\cos(4\pi(\sin\theta)/G)) \\ & + a_3(2 - 2\cos(2\pi(\cos\theta)/G)\cos(2\pi(\sin\theta)/G)) \\ & + a_4(0.5 - 0.5\cos(4\pi(\cos\theta)/G)\cos(4\pi(\sin\theta)/G)) \\ & + a_5(0.8 - 0.4\cos(4\pi(\sin\theta)/G + 2\pi(\cos\theta)/G) \\ & - 0.4\cos(2\pi(\sin\theta)/G - 4\pi(\cos\theta)/G)) \\ & + a_6(0.8 - 0.4\cos(2\pi(\sin\theta)/G + 4\pi(\cos\theta)/G) \\ & - 0.4\cos(4\pi(\sin\theta)/G - 2\pi(\cos\theta)/G)); \end{aligned}$$

$$\begin{aligned} M = {} & b_1 + b_2(2\cos(2\pi(\sin\theta)/G) + 2\cos(2\pi(\cos\theta)/G)) \\ & + b_3(2\cos(4\pi(\cos\theta)/G) + 2\cos(4\pi(\sin\theta)/G) \\ & + b_4(4\cos(2\pi(\cos\theta)/G)\cos(2\pi(\sin\theta)/G)) \\ & + b_5(4\cos(4\pi(\cos\theta)/G)\cos(4\pi(\sin\theta)/G)) \\ & + b_6(2\cos(4\pi(\sin\theta)/G + 2\pi(\cos\theta)/G) \\ & + 2\cos(2\pi(\sin\theta)/G - 4\pi(\cos\theta)/G)) \\ & + b_7(2\cos(2\pi(\sin\theta)/G - 4\pi(\cos\theta)/G) \\ & + 2\cos(4\pi(\sin\theta)/G - 2\pi(\cos\theta)/G)), \end{aligned}$$

where $G = \lambda/\Delta$ and G is the number of grid points per wavelength.

We can now calculate the numerical phase velocity $V_{ph} = \omega/k$ and the numerical group velocity $V_{gr} = \partial\omega/\partial k$: Equation (7) can be written as

$$\frac{V_{ph}}{v} = \frac{G}{2\pi}\sqrt{(L/M)}, \tag{8}$$

$$\frac{V_{gr}}{v} = \frac{1}{2\Delta}\frac{(M \times \partial L/\partial k - L \times \partial M/\partial k)/M^2}{\sqrt{(L/M)}}. \tag{9}$$

We have two ways to obtain the coefficients a_i and b_i. The first way is to minimize the error defined by the difference between the normalized phase velocity and unity (see Jo et al., 1996). The second approach, which we adopt here, is to explicitly assume the normalized phase velocity is unity for many propagation angles θ and many values of G simultaneously. If we attempt to satisfy this requirement for enough propagation angles, we obtain an overdetermined system of equations that can be solved in the least-squares sense. From equation (8), assuming unity, we obtain

$$\frac{G}{2\pi}\sqrt{L/M} = 1. \tag{10}$$

We rearrange equation (10) as

$$L - M4\pi^2/G^2 = 0 \tag{11}$$

and substitute the first constraint ($\sum_{i=1}^{6} a_i = 1$) associated with equation (6) to obtain

$$\tilde{L} + M4\pi^2/G^2 = 4, \tag{12}$$

where

$$\begin{aligned} \tilde{L} = {} & a_1(2\cos(2\pi(\sin\theta)/G) + 2\cos(2\pi(\cos\theta)/G)) \\ & + a_2(3 + 0.5(\cos(4\pi(\cos\theta)/G) + \cos(4\pi(\sin\theta)/G))) \\ & + a_3(2 + 2(\cos(2\pi(\cos\theta)/G)\cos(2\pi(\sin\theta)/G))) \\ & + a_4(3.5 + 0.5(\cos(4\pi(\cos\theta)/G)\cos(4\pi(\sin\theta)/G)) \\ & + a_5(3.2 + 0.4(\cos(4\pi(\sin\theta)/G + 2\pi(\cos\theta)/G) \\ & + \cos(2\pi(\sin\theta)/G - 4\pi(\cos\theta)/G))) \\ & + a_6(3.2 + 0.4(\cos(2\pi(\sin\theta)/G + 4\pi(\cos\theta)/G) \\ & + \cos(4\pi(\sin\theta)/G - 2\pi(\cos\theta)/G))). \end{aligned}$$

$$\begin{aligned} M = {} & b_1 + b_2(2\cos(2\pi(\sin\theta)/G) \\ & + 2\cos(2\pi(\cos\theta)/G)) \\ & + b_3(2\cos(4\pi(\cos\theta)/G) + 2\cos(4\pi(\sin\theta)/G)) \\ & + b_4(4\cos(2\pi(\cos\theta)/G)\cos(2\pi(\sin\theta)/G)) \\ & + b_5(4\cos(4\pi(\cos\theta)/G)\cos(4\pi(\sin\theta)/G)) \\ & + b_6(2\cos(4\pi(\sin\theta)/G + 2\pi(\cos\theta)/G) \\ & + 2\cos(2\pi(\sin\theta)/G - 4\pi(\cos\theta)/G)) \\ & + b_7(2\cos(2\pi(\sin\theta)/G + 4\pi(\cos\theta)/G) \\ & + 2\cos(4\pi(\sin\theta)/G - 2\pi(\cos\theta)/G)), \end{aligned}$$

where $G = \lambda/\Delta$ and G is the number of grid points per wavelength.

Because $\tilde{L}$ and M are functions of the number of grid points per wavelength G and the propagation angle θ, equation (12) can be given in a matrix form,

$$\begin{bmatrix} A_i^* & B_i^* & C_i^* & D_i^* & E_i^* & F_i^* & \cdot & \cdot & \cdot & K_i^* & L_i^* & M_i^* \\ \cdot & \cdot & \cdot & \cdot & \cdot & \cdot & \cdot & \cdot & \cdot & \cdot & \cdot & \cdot \\ \cdot & & & & & & & & & & & \\ \cdot & & & & & & & & & & & \\ \cdot & & & & & & & & & & & \\ \cdot & & & & & & & & & & & \\ \cdot & & & & & & & & & & & \\ \cdot & & & & & & & & & & & \\ \cdot & & & & & & & & & & & \\ \cdot & & & & & & & & & & & \\ A_n^* & B_n^* & C_n^* & D_n^* & E_n^* & F_n^* & \cdot & \cdot & \cdot & K_n^* & L_n^* & M_n^* \end{bmatrix}$$

$$\times \begin{bmatrix} a_1 \\ a_2 \\ a_3 \\ \cdot \\ \cdot \\ a_6 \\ b_1 \\ \cdot \\ b_6 \\ b_7 \end{bmatrix} = \begin{bmatrix} 4 \\ 4 \\ \cdot \\ \cdot \\ \cdot \\ \cdot \\ \cdot \\ \cdot \\ \cdot \\ \cdot \\ 4 \end{bmatrix}. \tag{13}$$

Each additional row is generated by choosing a new value of G or θ, where

$$A_k^* = 2\cos(2\pi \sin(\theta_i)/G_k) + 2\cos(2\pi \cos(\theta_i)/G_k),$$

$$B_k^* = 3 + 0.5\cos(4\pi \cos(\theta_i)/G_k) + \cos(4\pi \sin(\theta_i)/G_k),$$

$$C_k^* = 2 + 2\cos(2\pi \cos(\theta_i)/G_k)\cos(2\pi \sin(\theta_i)/G_k),$$

$$D_k^* = 3.5 + 0.5\cos(4\pi \cos(\theta_i)/G_k)\cos(4\pi \sin(\theta_i)/G_k),$$

$$E_k^* = 3.2 + 0.4(\cos(4\pi \sin(\theta_i)/G_k + 2\pi \cos(\theta_i)/G_k) + \cos(2\pi \sin(\theta_i)/G_k - 4\pi \cos(\theta_i)/G_k)),$$

$$F_k^* = 3.2 + 0.4(\cos(2\pi \sin(\theta_i)/G_k + 4\pi \cos(\theta_i)/G_k) + \cos(4\pi \sin(\theta_i)/G_k - 2\pi \cos(\theta_i)/G_k)),$$

$$G_k^* = 4\pi^2/G_k^2,$$

$$H_k = 4\pi^2/G_k^2(2\cos(2\pi \sin(\theta_i)/G_k) + 2\cos(2\pi \cos(\theta_i)/G_k)),$$

$$I_k^* = 4\pi^2/G_k^2(2\cos(4\pi \cos(\theta_i)/G_k) + 2\cos(4\pi \sin(\theta_i)/G_k)),$$

$$J_k^* = 4\pi^2/G_k^2(4\cos(2\pi \cos(\theta_i)/G_k)\cos(2\pi \sin(\theta_i)/G_k)),$$

$$K_k^* = 4\pi^2/G_k^2(4\cos(4\pi \cos(\theta_i)/G_k)\cos(4\pi \sin(\theta_i)/G_k)),$$

$$L_k^* = 4\pi^2/G_k^2(4\pi \cos(2\sin(\theta_i)/G_k + 2\pi \cos(\theta_i)/G_k) + 2\cos(2\pi \sin(\theta_i)/G_k - 4\pi \cos(\theta_i)/G_k)),$$

$$M_k^* = 4\pi^2/G_k^2(2\cos(2\pi \sin(\theta_i)/G_k + 4\pi \cos(\theta_i)/G_k) + 2\cos(4\pi \sin(\theta_i)/G_k - 2\pi \cos(\theta_i)/G_k)),$$

$$k = 1, \ldots, n, \quad i = 1, \ldots, m.$$

As the number of grid points per wavelength (G) increases and the propagation angle with respect to the z-axis θ is changed, equation (13) becomes overdetermined. The number of rows in equation (13) is dependent on the number of grid points and the propagation angles chosen. In our case, the interval of propagation angle is 5° and the interval of $1/G$ is 0.0025. The maximum number of grid points is four points per wavelength ($G = 4$). The size of the overdetermined matrix is 1000 by 13. After solving the overdetermined matrix using the singular-value decomposition method, we obtained the coefficients below.

$$a_1 = 0.0949098, \quad a_2 = 0.280677, \quad a_3 = 0.247253,$$
$$a_4 = 0.0297441, \quad a_5 = 0.173708, \quad a_6 = 0.173708,$$
$$b_1 = 0.363276, \quad b_2 = 0.108598, \quad b_3 = 0.00414870,$$
$$b_4 = 0.0424801, \quad b_5 = 0.000206312,$$
$$b_6 = 0.00187765, \quad b_7 = 0.00188342. \tag{14}$$

Figure 3 shows normalized phase and group velocity curves based on these coefficients. If we require the normalized group velocity to be less than 0.5%, the conventional five-point formula in the frequency domain requires $G = 13$ (Figure 4). For a comparable degree of accuracy, the optimal nine-point formula of Jo et al. (1996) requires $G = 5$ (Figure 5). For the 25-point average finite-difference operator, the number of grid points per shortest wavelengths is 2.5 (Figure 3). The new scheme offers a substantial reduction (50%) in the number of grid points while maintaining the same bandwidth of the complex impedance matrix. Consider the total number of core elements required to store the complex impedance matrix when we use the band matrix solver to factor the complex impedance matrix. Suppose that the number of computer core locations used to store the complex impedance matrix for the 9 point scheme for $G = 5$ is $N_x \times N_z \times N_z$, where N_x is the number of grid points in the x-direction and N_z is the number of grid points in the z direction. The number of core memory elements for the twenty five scheme for $G = 2.5$ will be $(N_x/2) \times (N_z/2) \times (N_z)$. This results in a memory reduction of one quarter and maintenance of the same bandwidth, N_z, and results in the reduction of floating point operations by four when a scalar computer is used to factor the complex impedance matrix.

NUMERICAL EXAMPLE

To test the frequency-domain code based on the twenty-five point scheme, we used a 2-D homogeneous model (2000 m × 2000 m) as shown in Figure 6. The source is located at a subsurface point and the receiver is located 1000 m horizontally from the source. The velocity of the medium is 1500 m/s, and the highest frequency used is 75 Hz. The grid interval is 10 m for the minimum number of grid points (i.e., two points per wavelength) allowed. For 200 × 200 mesh points, we

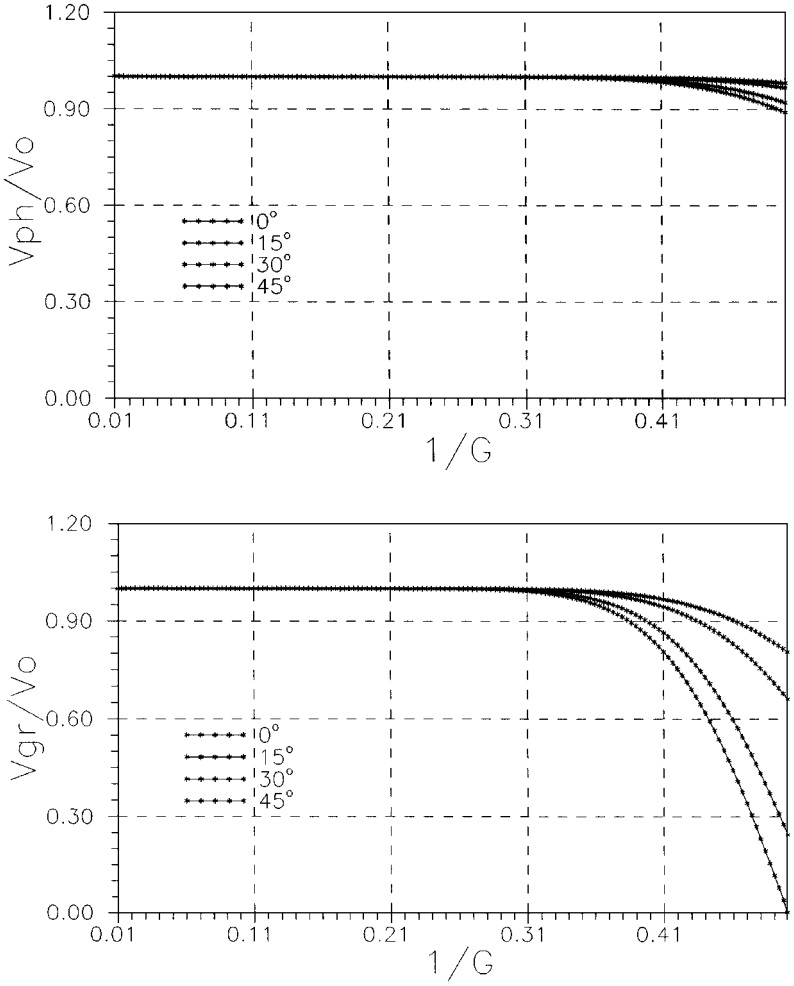

FIG. 3. Normalized phase and group velocity curves for the finite-difference solution of the 2-D scalar wave equation in the frequency domain using a 25-point weighted-average difference formulation with the coefficients given in the text.

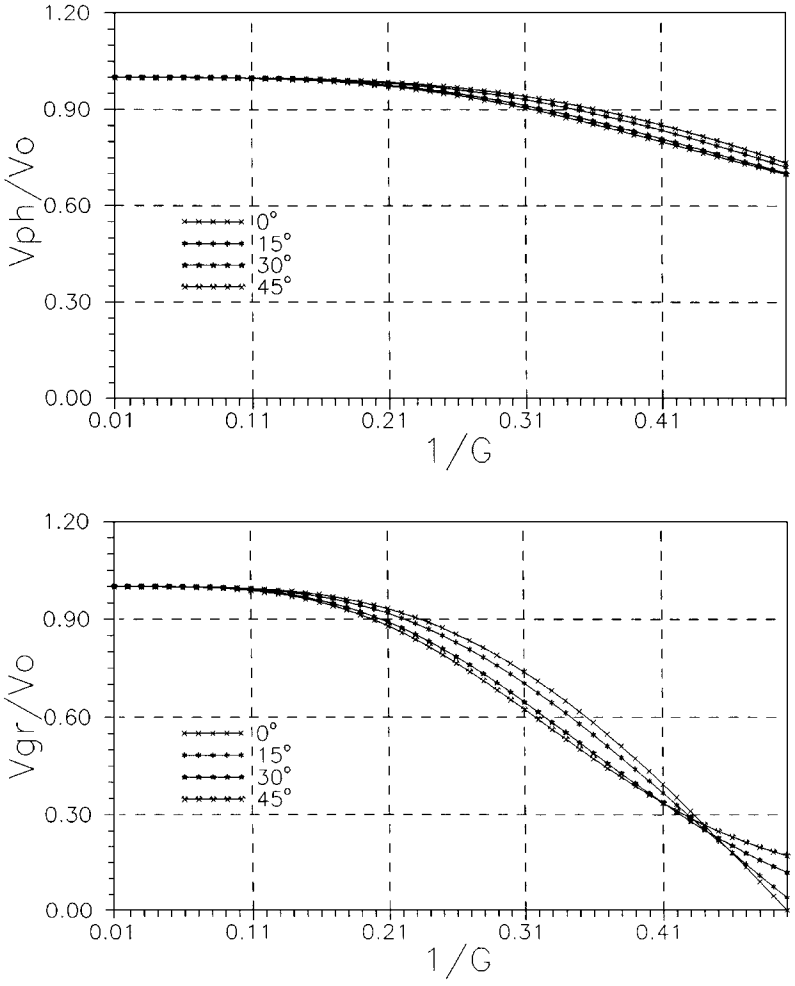

FIG. 4. Normalized phase and group velocity curves for different propagation angles with respect to the grid, for the finite-difference solution of 2-D scalar wave equation using a conventional five-point difference formulation in frequency-space domain.

generated synthetic seismograms by the conventional five-point formula of Pratt and Worthington (1990), nine-point formula of Jo et al. (1996), and the twenty five point formula of this study. Figure 7 shows the synthetic seismograms for each formulation. As shown in Figure 7, the synthetic seismograms based on the five- and nine-points formulas suffer from more grid dispersion than the twenty-five-point formula.

CONCLUSIONS

We have developed a new frequency-domain finite-difference scheme by extending the difference star at the collocation point. The new scheme offers a substantial reduction in the number of grid points and extra savings of core memory, while maintaining the same bandwidth of the complex impedance matrix. In terms of the group velocity, the new scheme is comparable to the pseudospectral method (Kosloff and Baysal, 1982). The consequence of this reduced storage is that realistically sized models can now be used in the space-frequency domain, making multisource modeling and inversion possible for large scale exploration problems.

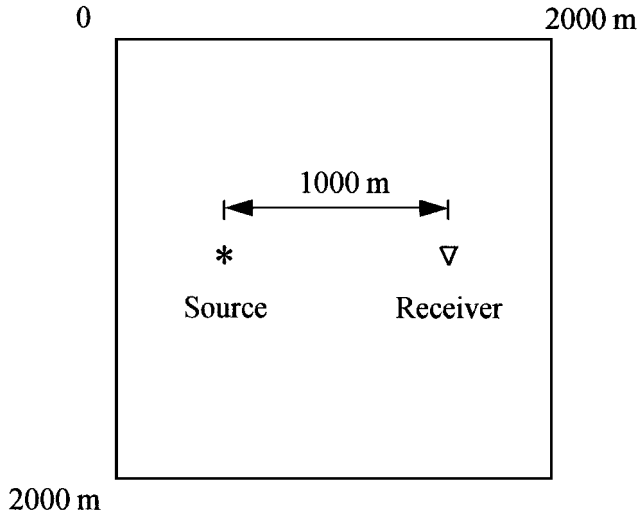

FIG. 6. The homogeneous model taken to compare the synthetic seismograms by each different method.

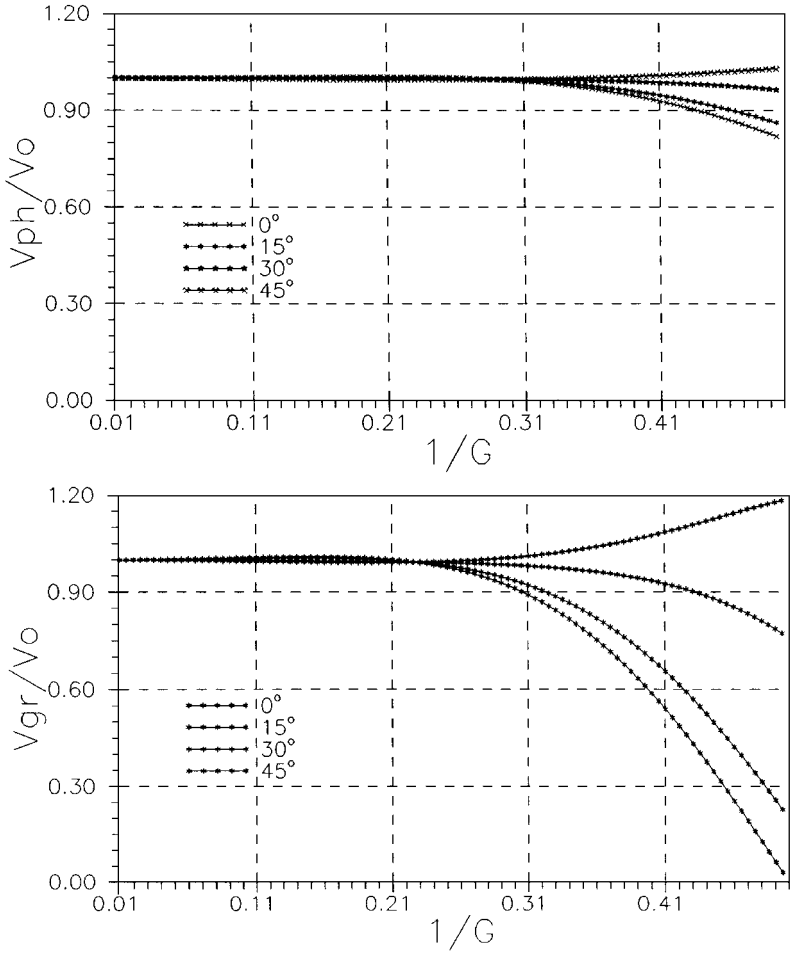

FIG. 5. Normalized phase and group velocity curves for the frequency-domain finite-difference solution using the nine point weighted average difference formulation given in Jo et al. (1996).

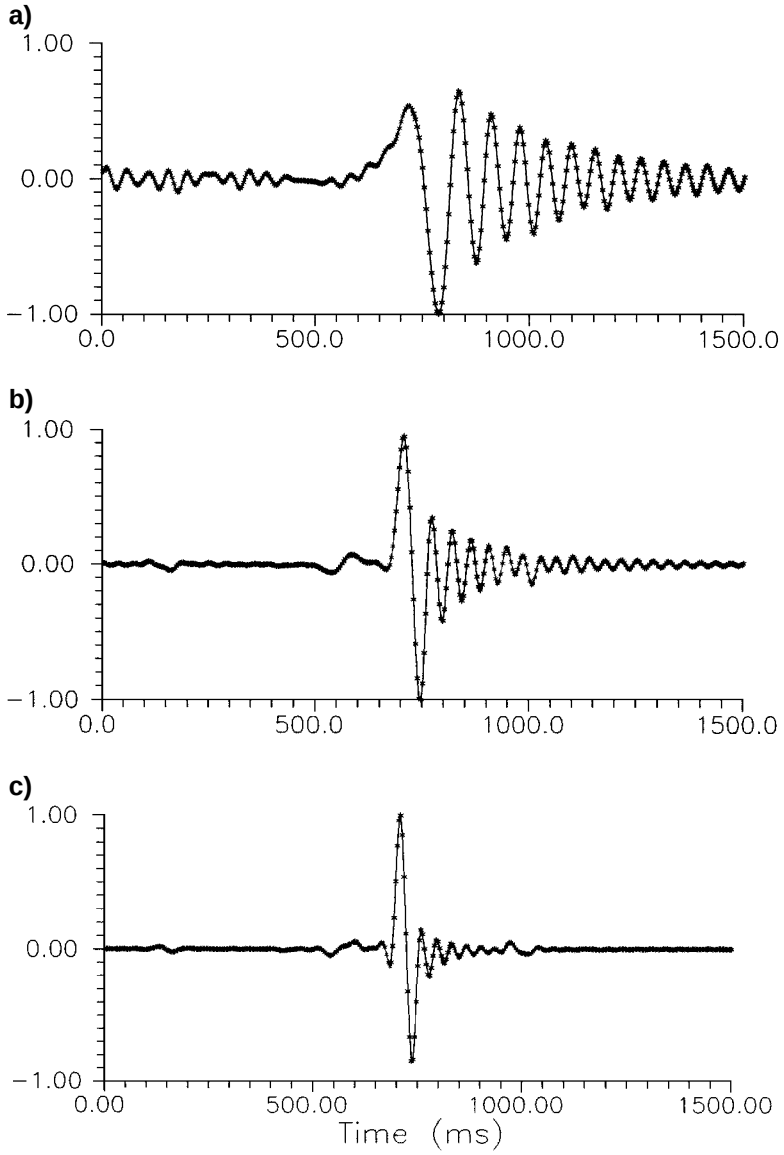

FIG. 7. Synthetic seismograms generated by the different finite-difference technique using two-grid points per wavelength in all cases ($G = 2$). (a) Synthetic seismogram generated by the conventional five-point difference star. (b) Synthetic seismogram generated by the nine-point finite-difference star of Jo et al. (1996). (c) Synthetic seismogram generated by the twenty-five point operator of this study.

ACKNOWLEDGMENTS

We thank Dr. K. J. Marfurt and Dr. K. R. Kelly of Amoco Production Company and Professor Gerhard Pratt of Imperial College of University of London for their fruitful discussions during this study. Also we wish to thank anonymous reviewers for their constructive comments on this paper.

REFERENCES

Alford, R. M., Kelly, K. R., and Boore, D. M., 1974, Accuracy of finite-difference modeling of the acoustic wave equation: Geophysics, **39**, 834–842.

Dablain, M. A., 1986, The application of high-order differencing to the scalar wave equation: Geophysics, **51**, 54–66.

Jo, C. H., Shin, C. S., and Suh, J. H., 1996, An optimal nine-point finite-difference frequency-space 2-D acoustic wave extrapolator: Geophysics, **61**, 529–537.

Kosloff, D. D., and Baysal, E., 1982, Forward modeling by a fourier method: Geophysics, **47**, 1402–1412.

Marfurt, K. J., 1984, Accuracy of finite-difference and finite-element modeling of the scalar and elastic wave equations: Geophysics, **49**, 533–549.

Pratt, R. G., and Worthington, M. H., 1990, Inverse theory applied to multi-source cross-hole tomography Part I : Acoustic wave-equation method: Geophys. Prosp., **38**, 287–310.